SUPPLEMENTAL MATERIAL

Loss of SPEG Inhibitory Phosphorylation of RyR2 Promotes Atrial Fibrillation

Hannah M. Campbell BS, Ann P. Quick PhD, Issam Abu-Taha PhD, David Y. Chiang MD, PhD, Carlos F. Kramm PhD, Tarah A. Word PhD, Sören Brandenburg PhD, Mohit Hulsurkar PhD, Katherina M. Alsina, PhD, Hui-Bin Liu PhD, Brian Martin PhD, Oliver M. Moore BS, Satadru K. Lahiri PhD, Eleonora Corradini PhD, Markus Kamler MD PhD, Albert J.R. Heck PhD, Stephan E. Lehnart MD, Dobromir Dobrev MD, Xander H.T. Wehrens MD, PhD

Expanded Methods

Animal Models. All mouse studies were performed according to the protocols approved by the Baylor College of Medicine Institutional Animal Care and Use Committee and conform to the Guide for the Care and Use of Laboratory Animals published by the US National Institutes of Health. Mice were provided standard chow and bedding by the Center for Comparative Medicine at Baylor College of Medicine. All experiments using mice were performed in a blinded manner. A cardiomyocyte-specific SPEG conditional knock-out (SPEG cKO) mouse was generated by crossing $SPEG^{fl/fl}$ mice on a C57/Bl6N background provided by KOMP to tamoxifen-inducible Myh6-mER-Cre-mER (MCM) mice purchased from Jackson Laboratories (stock number 011038) as described.[15] Male SPEG cKO mice and MCM control mice were intraperitoneally injected with 100 µL of 10 mg/mL tamoxifen for 3 consecutive days to induce Cre expression.

An atrial-specific SPEG conditional knock-out mouse (SPEG aKO) was generated by injecting 2-3 month-old $SPEG^{fl/fl}$ mice with AAV9-ANF-Cre at a dose of $1x10^{12}$ genome copies for biochemistry and *in vivo* experiments. Wild-type (WT) littermates were injected with AAV9-ANF-Cre as controls. The atrial specificity of this virus was previously validated by Li *et al.*[40] Both male and female mice were included in all experiments with SPEG aKO mice. For studies involving confocal microscopy, $SPEG^{fl/fl}$ and WT

mice were injected with ANF-Cre-2a-mCherry-WPRE at a dose of $5x10_{11}$ genome copies/mouse to mark successfully transduced atrial myocytes with a red fluorescent protein.

RyR2-S2367A (phospho-resistant) and RyR2-S2367D (phospho-mimetic) mice were generated using CRISPR-Cas9 with cytosolic Cas9 protein embryo microinjections. Mice were generated on a C57/Bl6J background supplied by Jackson Laboratories (stock number: 000664) and backcrossed for at least two generations prior to being used in experiments. All studies were performed in both male and female mice with WT littermates as controls.

Western Blotting. Mice were anesthetized using 2.0% isoflurane in 100% oxygen. After adequate levels of anesthesia were confirmed by a toe pinch, mice were euthanized by cervical dislocation. Explanted hearts were dissected and flash frozen in liquid nitrogen. Atrial and ventricular lysates were obtained following homogenization in RIPA lysis buffer with 10% CHAPS (3-[(3-cholamidopropyl) dimethylammonio]-1-propanesulfonate; Sigma-Aldrich, St. Louis, MO; 331717-45-4) and phosphatase and protease inhibitors, PhosSTOP and cOmplete (ROCHE, Basel, Switzerland; 1836153001 and 4906845001), followed by sonication for 3 x1 s. Lysates were denatured in 2x Laemmli buffer (Biorad, Hercules, CA; 1610737) for 30 minutes at room temperature followed by electrophoresis on acrylamide gels (4% stacking, 6 and 12% resolving gradient). Protein was transferred to PVDF membranes overnight at 4°C, followed by 30-minute block (Prometheus OneBlock, Geneseesci, San Diego, CA; 20-314) and primary antibody incubation at either 4°C (overnight) or room temperature (3 hours). Primary antibodies used: mouse-anti-RyR2 (Invitrogen, Carlsbad, CA; catalogue # MA3-916, 1:2000), custom rabbit-anti-RyR2-pS2814 (YenZym, South San Francisco, CA; 1:1000), custom RyR2-pS2367 (YenZym, South San Francisco, CA, 1:200), rabbit-anti-RyR2-pS2808 (Abcam, Cambridge, United Kingdom, ab59225, 1,10:000), rabbit-anti-SPEG (Sinobiological, Beijing, China; 12472-T16; 1:500), mouse-anti-GAPDH (EMD Millipore, Burlington, MA; AB2302; 1:10,000), Membranes were washed three times, followed by incubation for 1-2 hours at room temperature with secondary antibodies for mouse (Alexa Fluor 488 goat-anti-mouse, Abcam, Cambridge, United Kingdom; A28175; 1:10,000) or rabbit (DyLight 800 goat-anti-rabbit, Rockland, Limerick, PA; 611-145-002; 1:10,000). Imaging was performed using a Li-Cor Odyssey

Blot Imager with analysis performed in ImageJ software. For human atrial samples, stratified randomization was performed to best control for clinical co-variates. Western protocols on flash frozen biopsies were the same as those done for mouse tissue above.

Programmed Electrical Stimulation. Programmed stimulation was performed as reported previously.[21] Mice were anesthetized using 2.0% isoflurane in 100% O_2 (1.0 L per minute). A 1.1F octapolar electrode catheter (EPR-800, Millar Instruments, Houston, TX) was inserted into the right ventricle via the right jugular vein. Data was acquired using a computer-based system (Emka Technologies, Falls Church, VA) and data was recorded via a 6-lead surface ECG and 4 intracardiac bipolar electrograms. Pacing was performed in the right atria through 2-ms current pulses with an external stimulator (STG-3008, MultiChannel Systems, Reutlingen, Germany). Electrophysiological data for sinus node refractory time (SNRT) and atrial ventricular node effective refractory period (AVERP) were obtained by standard clinical pacing protocols. Atrial fibrillation (AF) susceptibility was determined using rapid atrial burst pacing. This protocol was repeated three times. A mouse was considered positive for AF if it had at least 2 AF episodes greater than 1 second each. Mice were humanely euthanized following the procedure. The percentage of positive mice in each group was reported as the AF inducibility.

For representative traces, electrophysiology data was imported into MATLAB and filtered using a method based on wavelets transform with a sampling frequency of 200 Hz and a cut-off frequency of 5 Hz corresponding to a mouse rate of 300 bpm.[45] The AHA recommendation is a cut-off frequency of 0.67 Hz corresponding to a human heart rate of 40 bpm; we adjusted this frequency to better reflect mouse physiology. The program used was adapted from code provided at https://github.com/fperdigon/ECG-BaseLineWander-Removal-Methods.

Cloning of ANF-Cre-2A-mCherry-WPRE. Plasmid AAV9-ANF-CRE was constructed as reported earlier.[40] To enable identification of atrial cardiomyocytes with SPEG knockdown, an additional mCherry sequence was added. A 2A peptide sequence was added between Cre and mCherry for bicistronic

expression of both genes.[46] mRNA translation efficiency was enhanced through addition of woodchuck hepatitis virus (WHP) post-transcriptional regulatory element (WPRE) to recruit more ribosomes.[47]

Cellular Ca^{2+} imaging and analysis. Isolated myocytes were loaded with 2 mM Fluo-4-AM (Invitrogen, Carlsbad, CA) in normal Tyrode buffer solution (pH = 7.4 ± 0.05) containing 1.8 mM Ca^{2+} and prepared for Ca^{2+} sparks imaging as described.[15] Briefly, Ca^{2+} sparks were recorded using line-scan mode with 1024 pixels per line at 500 Hz on a LSM880 confocal microscope (Carl Zeiss, Thornwood, NY). Images were collected using a Zeiss Axiocam 503 mono camera using Zen Black Software. For cells from mice with AAV9-ANF-Cre-2a-mCherry-WPRE, transduction efficiency was determined by counting the percentage of mCherry-positive atrial myocytes identified by morphology and striations at 10x magnification. Cells that had a >20% increase in red signal compared to non-transfected control cardiomyocytes were considered positive for mCherry expression. 1-Hz steady-state Ca^{2+} transient pacing of the myocytes was induced followed by an ~20 second pause during which sparks were recorded. Only cells that contracted at 1-Hz were included in the study. Ca^{2+} transient amplitude (CaT) was quantified by normalizing peak fluorescence to basal fluorescence using Clampfit. Additionally, sarcoplasmic reticulum (SR) Ca^{2+} load was measured as peak fluorescence to basal fluorescence after pacing followed by acute caffeine application (~10 mM) to release SR Ca^{2+}.

Ca^{2+} spark properties were analyzed using the SparkMaster plugin in ImageJ (NIH). First, a region approximately 5 seconds long was selected approximately 3 seconds from the last paced Ca^{2+} transient and analysis was performed on this segment using the “shift+D” function. The scanning speed was set to 813.00 scan lines per second, Pixel size was 0.100 μm, background fluorescence was 0, criteria was set to filter out anything 3.8x the SD, and number of intervals was set to 1. Extended kinetics mode was used to analyze sparks and spark parameters. False positive sparks were further filtered out using the criteria in **Table I**. Spark images were obtained through SparkMaster by setting the output image to F/F0. Then the heat map.lut plugin in imageJ was used display the sparks dimensions using a heatmap (low=blue, mod=white, high=red). To test for differences in ryanodine sensitivity of individual RyR2 channels, atrial myocytes isolated from WT and S2367A mice were incubated in Fluo4-AM. After cells

were paced at 1 Hz to determine viability, cells were treated with 50 nM ryanodine (Sigma Aldrich, St. Louis, Missouri United States, Catalog #559276). At this dose, only a small percentage of RyR2 channels are bound to ryanodine.[20] Thus, it is unlikely that two channels in the same cluster would be bound to ryanodine. Cells were paced again at the end of the experiment to assess survival and to assure that cells did not migrate during the course of the experiment. Cells that failed to follow pacing were excluded from the study. Sparks were sorted by RyR2 cluster and time using the output coordinates generated by the spark master plugin on ImageJ software.

Immunofluorescence STED nanoscopy. Atrial cardiomyocytes were isolated from 8-12 weeks old male WT mice on a C57BL/6J background using a modified Langendorff perfusion protocol. Initially, mouse hearts were perfused with nominally Ca^{2+} free buffer (in mM: NaCl 120.4, KCl 14.7, KH_2PO_4 0.6, Na_2HPO_4 0.6, $MgSO_4$ 1.2, HEPES 10, $NaHCO_3$ 4.6, taurine 30, 2,3-butanedione-monoxime 10, glucose 5.5, pH 7.4 with NaOH), followed by collagenase type II (Worthington) containing buffer for cardiac tissue collagen digestion. Isolated atrial myocytes were plated on laminin coated coverslips and fixed with 4% PFA for 5 min. After incubation in blocking/ permeabilization buffer overnight (10 % bovine calf serum and 0.2 % Triton in PBS), myocytes were incubated with primary antibodies in blocking buffer at 4°C overnight as follows: SPEG 1:500 (12472-T16, SinoBiological, Beijing, China); RyR2 1:500 (MA3-916, Thermo Fisher Scientific, Waltham, MA). Next, samples were washed in blocking buffer and incubated with secondary antibodies diluted 1:1,000 for 2 h at room temperature: goat anti-rabbit STAR 635P (2-0012-007-2, Abberior, Göttingen, Germany) and goat anti-mouse STAR 580 (2-0002-005-1, Abberior, Göttingen, Germany). After washing in PBS, samples were embedded in mounting medium (ProLong Gold Antifade Mountant, Thermo Fisher Scientific, Waltham, MA). For imaging, we used a Leica TCS SP8 STED system with a HC PL APO C2S 100x/1.40 oil immersion objective. STED images were acquired using a pixel size of 16.23 x 16.23 nm, a pixel dwell time of 400 ns, a scanning speed of 600 Hz, 32x line averaging, fluorophore excitation by a white-light laser at 635 and 580 nm, STED depletion at 775 nm, and fluorescence detection between 650-700 nm and 600-630 nm. The STED laser beam was adjusted to optimize the STAR 635P and STAR 580 signal resolutions. Raw images were processed

in ImageJ, and line profiles were plotted in GraphPad Prism 7.03. For co-localization analysis, intracellular ROIs excluding the subsurface SPEG/RyR2 signals were manually selected, and immunofluorescence signal patterns of SPEG and RyR2 were segmented by automated ImageJ operations: background subtraction (rolling ball radius 25/35 pixels for SPEG/RyR2), smoothing (Gaussian, sigma 1 pixel), local contrast enhancement, and local Bernsen thresholding (radius 15 pixels). Binarized SPEG and RyR2 channels were used to determine the percentage of overlapping clusters and the relative overlap fraction for each channel. For overlap analysis we accepted clusters that ranged between partial up to mutually complete overlap in binarized images. Statistical analysis was based on the number of mouse hearts.

RyR2-immunoprecipation and mass spectrometry. Adult $SPEG_{fl/fl}$ mice were injected with 100 µL of 10 mg/mL tamoxifen (Sigma Aldrich, St. Louis, MO, T5648) for 3 days intraperitoneally. Hearts were harvested and flash frozen in liquid nitrogen to preserve phosphorylation. Hearts were pulverized using the CellCrusher (Kisker Biotech, Steinfurt, Germany; 538003) and resuspended by vortexing in RIPA lysis buffer containing Phosstop and cOmplete mini, NaF (Sigma-Aldrich, St. Louis, MO; S7920), Na_3VO_4 (Sigma-Aldrich, St. Louis, MO; S6508), and 1% CHAPS detergent. Samples were sonicated 3x for 1 s each and centrifuged at 16,000 g for 25 min at 4◦C.

Supernatants were then diluted in Lysis buffer and 1mL (6 mg) protein was used for immunoprecipitation. Lysates were precleared using 40 µL Protein G agarose beads (Pierce, Waltham, MA; S6508) for 2 hrs at 4_0C. Samples were centrifuged at 2,000 rpm at 4◦C and supernatant was collected for coimmunoprecipitation. Supernatants were incubated by rotating at 4◦C with 10 µL RyR2 antibody (Invitrogen, Carlsbad, CA; MA3-916) overnight. Fresh protein G agarose beads were washed in PBS and resuspended in modified RIPA lysis buffer. 100 µL of bead /RIPA slurry was added to each sample and rotated at 4◦C 1.5hr.

Samples were spun down at 2,000 rpm at 4◦C and supernatants were removed without disturbing the beads. A modified RIPA wash buffer with the same composition as the lysis buffer with the exception that the CHAPS was reduced to 0.5% was used to wash the beads containing the immunoprecipitates.

Beads were washed twice with 1 mL wash buffer by inverting tube beads in wash buffer 3x. All the supernatant was removed and immunoprecipitates were incubated in 30 μL 2x Laemmli sample buffer containing 5% beta mercaptoethanol for 10 minutes at 70°C. Denatured immunoprecipitates were then shipped on dry ice to the Netherlands for mass spectrometry.

Immunoprecipitates were separated on a tris-acetate gel (Bio-Rad) and the band at ~565 kDa, corresponding to the RyR2 was excised from the gel, and trypsin digestion was performed according to standard procedures. LC-MS/MS was performed on an Orbitrap QExactive.The raw data files were analysed with Proteome Discoverer (version 1.3, Thermo Scientific, Bremen, Germany) using Uniprot mouse FASTA database. Carbarmidomethylation of cysteines was set as fixed modification, oxidation of methionine and phosphorylation (S, T, Y) were used as variable modification. Phosphorylation sites were localized by applying phosphoRS (pRS) (v2.0). The phosphorylated peptides were normalized to the total number of RyR2 peptides.

Table I. Inclusion Criteria for Ca_{2+} Sparks

	F/F0	FWHM	FDHM	FullWidth	FullDur	TtP	Dvdt	tau
cut-off low	0.1	0.5	10	1	10	5	6	6
cut-off high	NA	10	100	11.6	200	100	100	150

Table II. Paroxysmal AF Patient Characteristics

	NSR	pAF
Patients, n	30	27
Gender, M/F	13/17	22/5
Age, y	70.9±1.7	70.9±1.6
Body mass index, kg/m2$	29.1±1.3	29.4±1.0
CAD, n (%)	5 (17)	11 (41)
AVD/MVD, n (%)	20 (67)	11 (41)
CAD+AVD/MVD, n (%)	5 (17)	5 (19)
Hypertension, n (%)	23 (77)	23 (85)
Diabetes, n (%)	8 (27)	12 (44)
Hyperlipidemia, n (%)	10 (33)	12 (44)
LVEF, %§	60.5±1.1	56.5±1.9
LA, mm#	42.4±1.1	45.8±1.5
P wave duration, ms†	82.1±3.6	76.1±4.1
Time since last AF episode, days; median (range)‡	-	10 (1-784)
Digitalis, n (%)	0 (0)	1 (4)
ACE inhibitors, n (%)	10 (33)	11 (41)
AT1 blockers, n (%)	6 (20)	7 (26)
β-Blockers, n (%)	18 (60)	22 (81)
Dihydropyridines, n (%)	7 (23)	6 (22)
Diuretics, n (%)	10 (33)	12 (44)
Nitrates, n (%)	1 (3)	0 (0)
Lipid-lowering drugs, n (%)	11 (37)	17 (63)

NSR, normal sinus rhythm as control; pAF, paroxysmal atrial fibrillation; CAD, coronary artery disease; AVD, aortic valve disease; MVD, mitral valve disease; LVEF, left ventricular ejection fraction; LA, left atrial diameter; ACE, angiotensin converting enzyme; AT, angiotensin receptor. Fisher's exact test used

for categorical variables. Unpaired t test or Mann-Whitney test used for continuous variables. $Data were not available for 1 SR. §Data were not available for 4 SR, 1 pAF. #Data were not available for 9 SR, 12 pAF. †P wave was absent in 5 pAF patients because ECG recorded during AF.

Table III. Characteristics of pAF Patients Used for SPEG Detection

	NSR	pAF
Patients, n	22	23
Gender, M/F	9/13	19/4
Age, y	70.4±2.2	70.4±1.7
Body mass index, kg/m$_2$	29.3±1.6	28.9±1.0
CAD, n (%)	5 (24)	9 (39)
AVD/MVD, n (%)	13 (62)	10 (43)
CAD+AVD/MVD, n (%)	3 (14)	4 (17)
Hypertension, n (%)	18 (82)	19 (83)
Diabetes, n (%)	5 (23)	9 (39)
Hyperlipidemia, n (%)	8 (36)	10 (43)
LVEF, %§	60.4±1.3	55.3±2.1
LA, mm#	42.1±1.3	45.5±1.4
P wave duration, ms†	84.9±3.8	73.9±4.2
Time since last AF episode, days; median (range)ǂ	-	10 (1-784)
Digitalis, n (%)	0 (0)	0 (0)
ACE inhibitors, n (%)	7 (32)	10 (43)
AT1 blockers, n (%)	5 (23)	6 (26)
β-Blockers, n (%)	13 (59)	19 (83)
Dihydropyridines, n (%)	4 (18)	4 (17)
Diuretics, n (%)	7 (32)	9 (39)
Nitrates, n (%)	1 (5)	0 (0)
Lipid-lowering drugs, n (%)	10 (45)	13 (57)

NSR, normal sinus rhythm as control; pAF, paroxysmal atrial fibrillation; CAD, coronary artery disease; AVD, aortic valve disease; MVD, mitral valve disease; LVEF, left ventricular ejection fraction; LA, left atrial diameter; ACE, angiotensin converting enzyme; AT, angiotensin receptor. Fisher's exact test used

for categorical variables. Unpaired t test or Mann-Whitney test used for continuous variables. §Data were not available for 3 SR. #Data were not available for 8 SR, 12 pAF. ǂData were not available for 7 pAF. †P wave was absent in 5 pAF patients because ECG recorded during AF.

.

Table IV. Chronic AF Patient Characteristics

	NSR	cAF
Patients, n	27	22
Gender, M/F	12/15	16/6
Age, y	71.0±1.8	71.3±1.5
Body mass index, kg/m2$	28.5±1.4	26.2±0.8
CAD, n (%)	5 (19)	3 (14)
AVD/MVD, n (%)	15 (56)	12 (55)
CAD+AVD/MVD, n (%)	7 (26)	7 (32)
Hypertension, n (%)	19 (70)	19 (86)
Diabetes, n (%)	7 (26)	5 (23)
Hyperlipidemia, n (%)	11 (41)	14 (64)*
LVEF, %§	58.7±1.9	51.2±2.4ǂ
LA, mm#	42.6±1.2	48.4±1.3ǂ
Digitalis, n (%)	0 (0)	9 (41)*
ACE inhibitors, n (%)	9 (33)	8 (36)
AT1 blockers, n (%)	6 (22)	7 (32)
β-Blockers, n (%)	16 (59)	16 (73)
Dihydropyridines, n (%)	5 (19)	6 (27)
Diuretics, n (%)	10 (37)	15 (68)*
Nitrates, n (%)	1 (4)	3 (14)
Lipid-lowering drugs, n (%)	11 (41)	14 (64)

NSR, sinus rhythm as control; cAF, chronic atrial fibrillation; CAD, coronary artery disease; AVD, aortic valve disease; MVD, mitral valve disease; LVEF, left ventricular ejection fraction; LA, left atrial diameter; ACE, angiotensin converting enzyme; AT, angiotensin receptor; *P<0.05 *versus* SR from Fisher's exact test for categorical variables. ǂP<0.05 *versus* SR from unpaired t test or Mann-Whitney test for continuous

variables. $Data were not available for 1 SR and 1 cAF. §Data were not available for 2 SR. #Data were not available for 8 SR, and 8 cAF.

Table V. Baseline ECG and Electrophysiology Parameters of SPEG aKO and WT mice

	WT (n=8)	SPEG aKO (n=10)
RR interval (ms)	120.6 ± 4.1	116.7 ± 5.8
PR interval (ms)	37.2 ± 0.6	36.3 ± 0.9
QRS interval (ms)	9.9 ± 0.4	9.7 ± 0.7
QT interval (ms)	24.4 ± 1.0	23.6 ± 0.7
SNRT (ms)	122.2 ± 5.4	123.5 ± 7.3
AVERP (ms)	72.1 ± 0.1	68.0 ± 0.9

Data analyzed with Krusal-Wallis. Data displayed as mean ± SEM

Table VI. Characteristics of pAF Patients Used for RyR2 Assessment

	NSR	pAF
Patients, n	21	20
Gender, M/F	8/13	18/2
Age, y	71.4±2.0	71.7±1.6
Body mass index, kg/m2$	29.5±1.7	29.5±1.2
CAD, n (%)	4 (19)	9 (45)
AVD/MVD, n (%)	15 (71)	6 (30)*
CAD+AVD/MVD, n (%)	2 (10)	5 (25)
Hypertension, n (%)	14 (67)	18 (90)
Diabetes, n (%)	4 (19)	9 (45)
Hyperlipidemia, n (%)	5 (24)	8 (40)
LVEF, %§	58.3±1.0	57.8±2.0
LA, mm#	43.1±1.5	45.1±1.7
P wave duration, ms†	81.9±4.5	75.4±4.8
Time since last AF episode, days; median (range)ǂ	-	10 (1-44)
Digitalis, n (%)	0 (0)	1 (5)
ACE inhibitors, n (%)	6 (29)	7 (35)
AT1 blockers, n (%)	4 (19)	4 (20)
β-Blockers, n (%)	12 (57)	17 (85)
Dihydropyridines, n (%)	5 (24)	6 (30)
Diuretics, n (%)	6 (29)	9 (45)
Nitrates, n (%)	1 (5)	0 (0)
Lipid-lowering drugs, n (%)	5 (24)	14 (70)*

NSR, sinus rhythm as control; pAF, paroxysmal atrial fibrillation; CAD, coronary artery disease; AVD, aortic valve disease; MVD, mitral valve disease; LVEF, left ventricular ejection fraction; LA, left atrial diameter; ACE, angiotensin converting enzyme; AT, angiotensin receptor. Fisher's exact test used for

categorical variables. *P<0.05 *versus* SR. Unpaired t test or Mann-Whitney test used for continuous variables. $Data were not available for 1 SR. §Data were not available for 3 SR. #Data were not available for 7 SR, 8 pAF. ǂData were not available for 7 pAF. †P wave was absent in 5 pAF patients because ECG recorded during AF.

Table VII. Baseline Echocardiography of RyR2-S2367 knock-in mice

	WT (n=10)	S2367A (n=11)	S2367D (n=5)
EF (%)	68.0 ± 1.9	69.9 ±1.8	69.8 ± 2.0
LVPW;d (mm)	0.75 ± 0.02	0.78 ± 0.02	0.72 ±0.03
LVPW;s (mm)	1.13 ± 0.04	1.14 ±- 0.04	1.05 ± 0.04
LVAW;d (mm)	0.73 ± 0.01	0.70 ± 0.03	0.76 ± 0.01
LVAW;s (mm)	1.12 ± 0.06	1.00 ± 0.07	1.04 ± 0.05
LVID;d (mm)	3.65 ±0.03	3.39 ± 0.07	3.71 ± 0.16
LVID;s (mm)	2.36 ± 0.05	2.29 ± 0.08	2.43 ± 0.16

WT, wild-type; EF: ejection fraction. LVPW: left ventricular posterior wall, LVAW: left ventricular anterior wall, LVID: left ventricular internal dimension, d: diastole, s: systole. Data displayed as mean ± SEM.

Table VIII. Baseline ECG and Electrophysiology Parameters of RyR2-S2367A and RyR2-S2367D knock-in mice

	WT (n=16)	S2367A (n=12)	S2367D (n=15)
RR interval (ms)	103.0 ± 1.7	104.2 ± 2.2	102.2 ± 1.7
PR interval (ms)	32.3 ± 0.8	33.2 ± 0.6	34.9 ± 0.5
QRS interval (ms)	8.8 ± 0.3	9.2 ± 0.2	9.3 ± 0.3
QT interval (ms)	19.8 ± 0.7	20.2 ± 0.7	21.4 ± 0.7
SNRT (ms)	117.5 ± 5.0	119.2 ± 4.3	110.6 ± 3.7
AVERP (ms)	65.9 ± 0.9	68.8 ± 4.7	66.6 ± 1.2

Data analyzed with Kruskal-Wallis. Data displayed at mean ± SEM

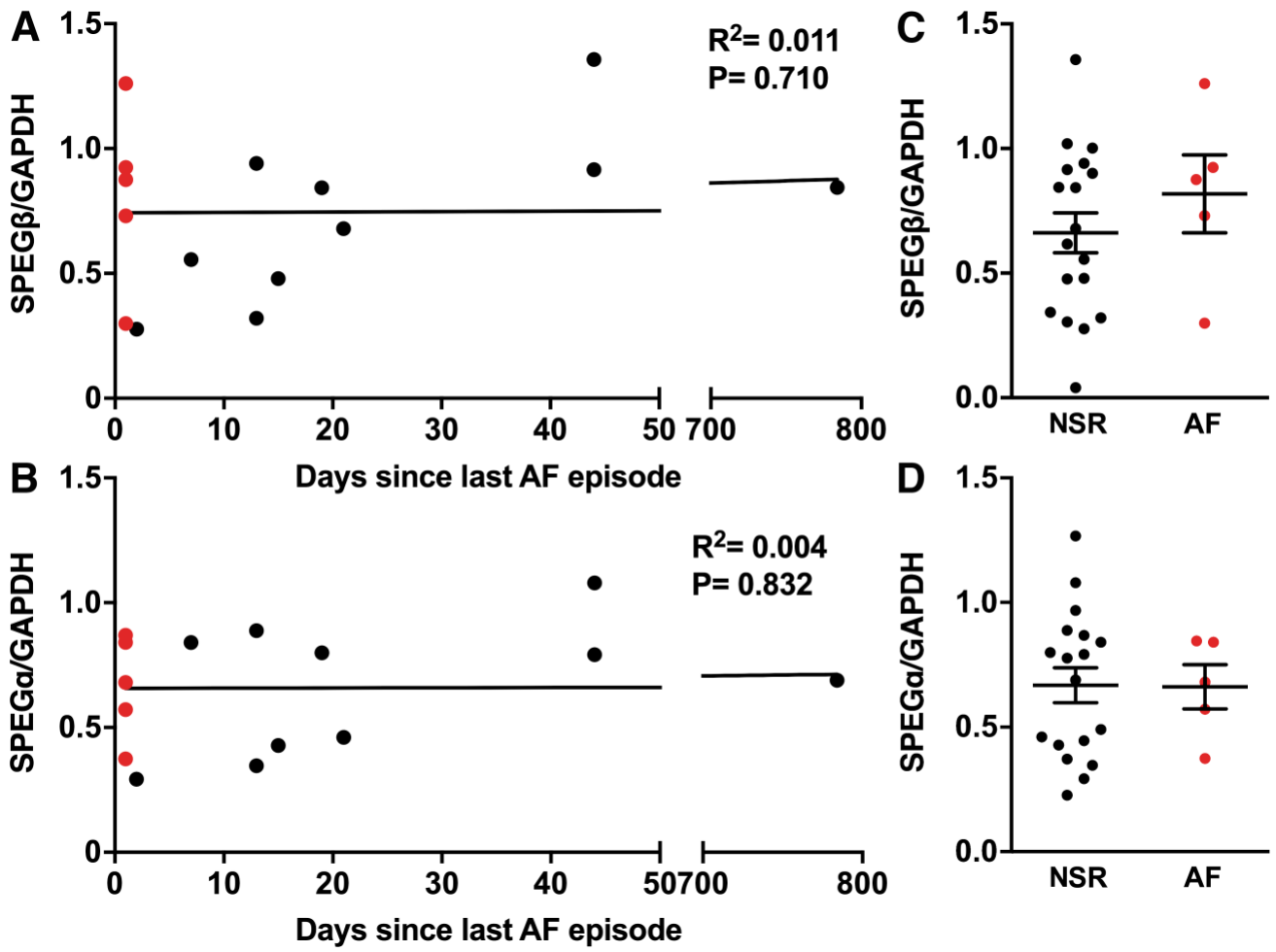

Figure I. Atrial SPEG levels in patients with paroxysmal AF are independent of the time interval between last documented AF episode and tissue collection during cardiac surgery. Scatter plots showing lack of correlation between days since last documented AF episode and SPEGβ (**A**) and SPEGα (**B**) levels (normalized to GAPDH) at time of cardiac surgery. Red dots mark patients with last AF episode <24 hours prior to surgery. Statistical analysis performed using Pearson correlation. (**C-D**) Dot plots showing lack of correlation between SPEGβ or SPEGα levels, respectively, and cardiac rhythm (SR or AF) at the time of the last ECG the day before surgery. NSR, normal sinus rhythm. Significance determined using Mann-Whitney U test.

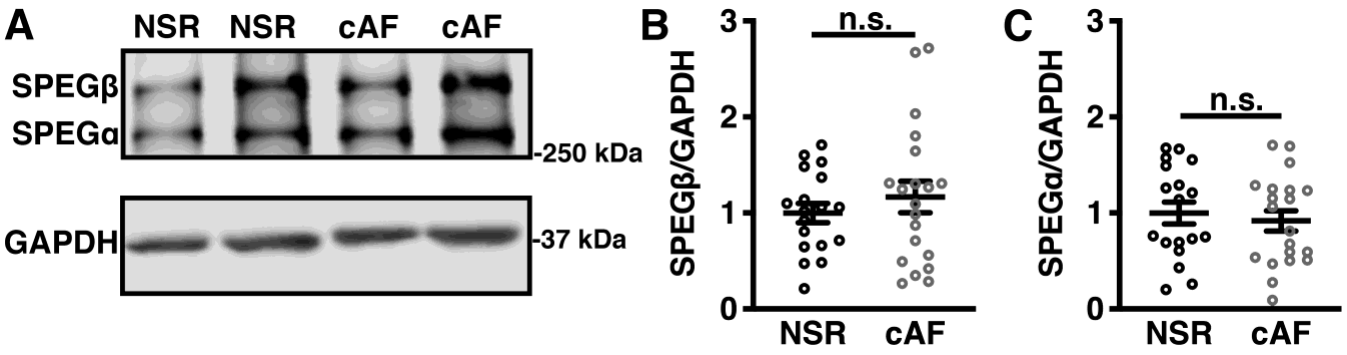

Figure II. Atrial SPEG protein levels are unchanged in patients with longstanding persistent (chronic) AF (cAF). Representative western blots (**A**) and bar graph quantifications of normalized (**B**) SPEGβ and (**C**) SPEGα protein levels relative to GAPDH as loading control in right-atrial appendage biopsies from patients in cAF or normal sinus rhythm (NSR). Statistical analyses performed using Student's t-test.

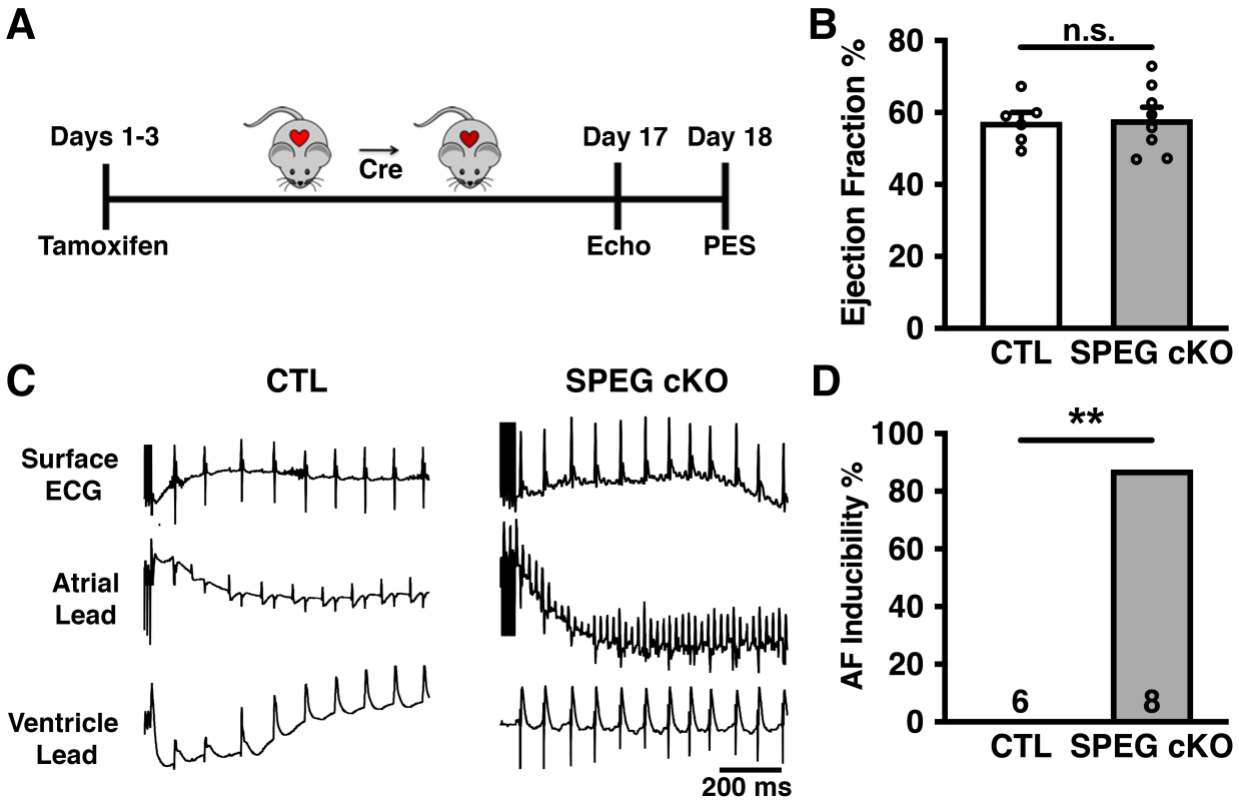

Figure III. SPEG cKO mice have enhanced susceptibility to AF. (**A**) 4-month-old mER-Cre-mER-SPEG$_{fl/fl}$ (SPEG cKO) and mER-Cre-mER control (CTL) mice were injected with tamoxifen for 3 days, followed by echocardiography (Echo) on day 17, and programmed electrical stimulation (PES) on day 18. (**B**) Bar graph demonstrating ejection fraction measured using echocardiography of CTL and SPEG cKO mice. Data were analyzed with the Mann Whitney-U test. Only mice with an ejection fraction greater than 45% were used for PES studies to avoid confounding effects of ventricular dysfunction. (**C**) Representative surface ECG traces and intracardiac electrograms mice after rapid atrial pacing from CTL maintaining normal sinus rhythm and SPEG cKO demonstrating AF. (**D**) Bar graph showing increased inducibility of AF in SPEG cKO mice. Data analyzed statistically with the Fisher's exact test. **P<0.01.

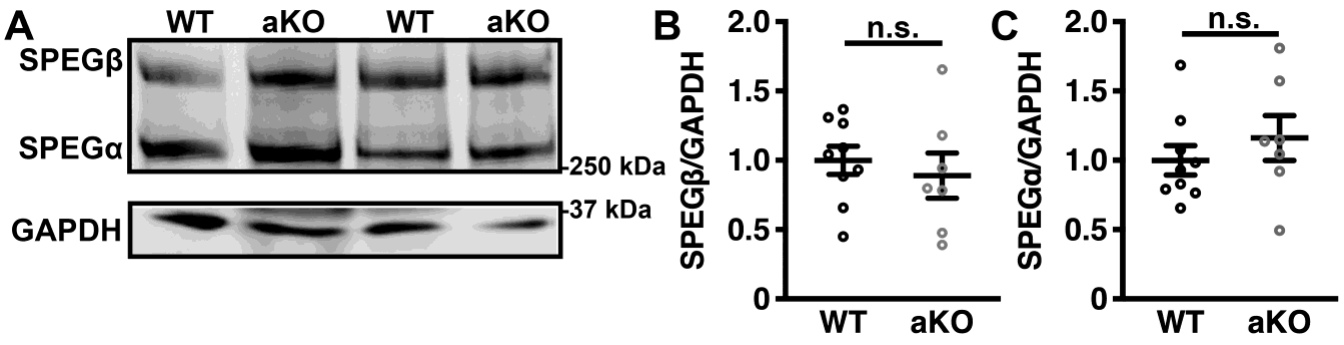

Figure IV. Unaltered ventricular SPEG levels in atrial-specific SPEG KO (aKO) mice. (**A**) Western blots of ventricular SPEG levels in SPEG aKO mice and WT controls three weeks after injection of AAV9-ANF-Cre. (**B-C**) Bar graphs showing quantification of ventricular SPEGα and SPEGβ levels in SPEG aKO mice and WT controls, normalized to GAPDH levels. Statistical analysis was performed using Mann-Whitney U test.

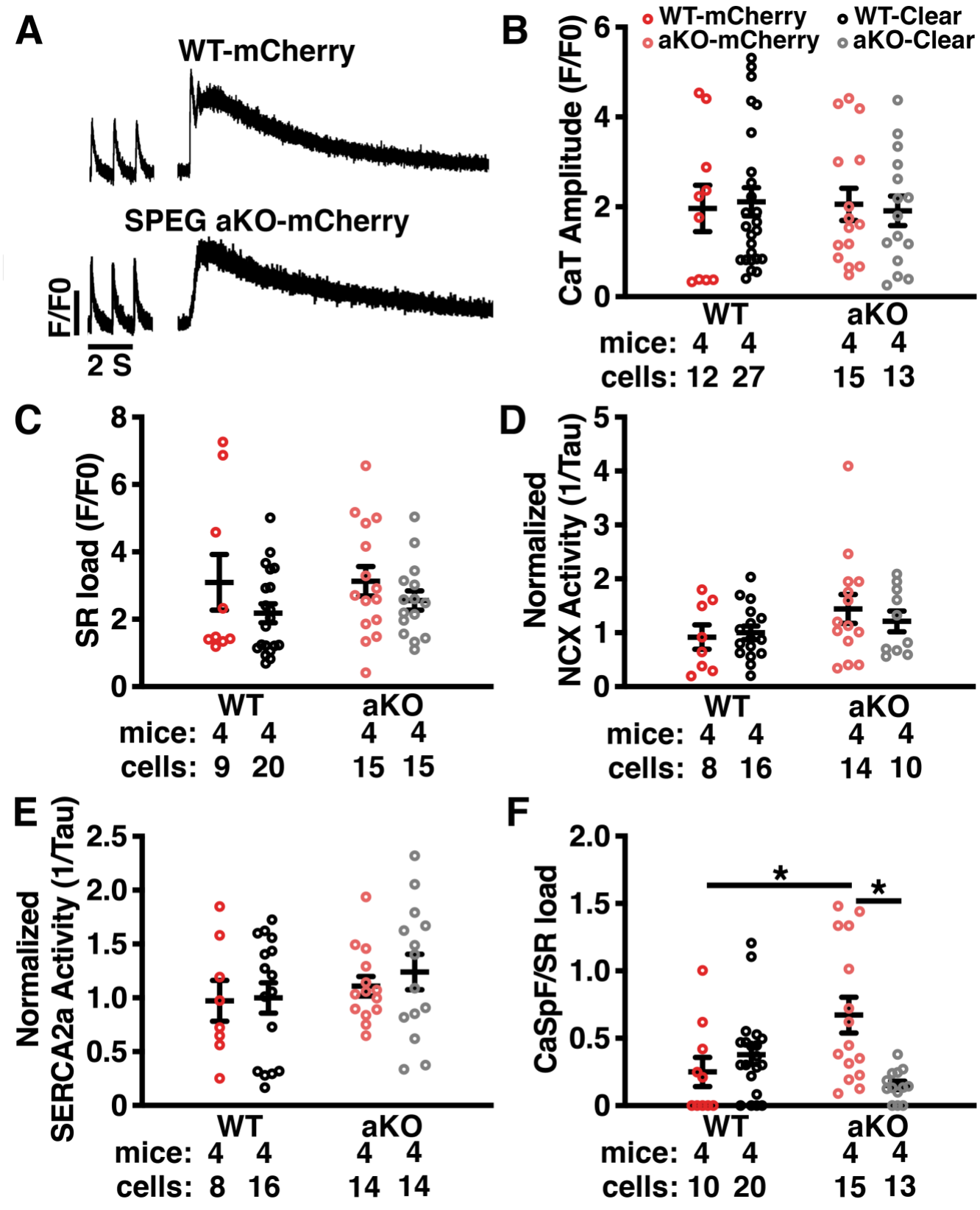
A
WT-mCherry
SPEG aKO-mCherry
F/F0
2 S
B
WT-mCherry
aKO-mCherry
WT-Clear
aKO-Clear
CaT Amplitude (F/F0)
WT
aKO
mice: 4 4 4 4
cells: 12 27 15 13
C
SR load (F/F0)
WT
aKO
mice: 4 4 4 4
cells: 9 20 15 15
D
Normalized NCX Activity (1/Tau)
WT
aKO
mice: 4 4 4 4
cells: 8 16 14 10
E
Normalized SERCA2a Activity (1/Tau)
WT
aKO
mice: 4 4 4 4
cells: 8 16 14 14
F
CaSpF/SR load
*
*
WT
aKO
mice: 4 4 4 4
cells: 10 20 15 13

Figure V. Unaltered Ca^{2+} transients in SPEG aKO myocytes. (A) Representative Ca^{2+} traces from mCherry positive WT and SPEG aKO mice. **(B)** Bar graph showing no change in Ca^{2+} transients (CaT). **(C)** Bar graph showing no change in SR Ca^{2+} loads between groups. **(D)** Bar graph showing no difference in NCX activity between groups as estimated by 1/Tau of SR Ca^{2+} load. **(E)** Bar graph showing no change in SERCA2a activity between groups as measured by 1/Tau of CaT after subtracting NCX activity. **(F)** Bar graph showing that CaSpF remains significant after normalizing to SR load. Statistical analyses performed with the generalized estimating equation. *P<0.05.

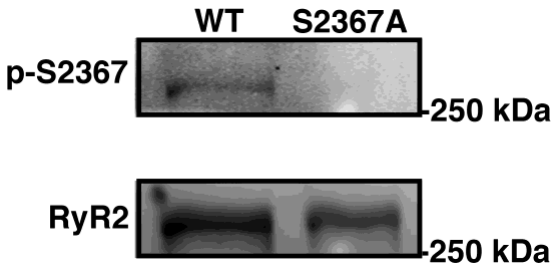

Figure VI. Validation of RyR2-S2367 phospho-specific antibody. Western blot of 100 μg WT and RyR2 S2367A mouse heart lysate. Immunoblot with 1:200 dilution custom RyR2-pS2367 antibody demonstrated antibody specificity for the RyR2 S2367 phosphorylation site. Total RyR2 was used as a loading control.

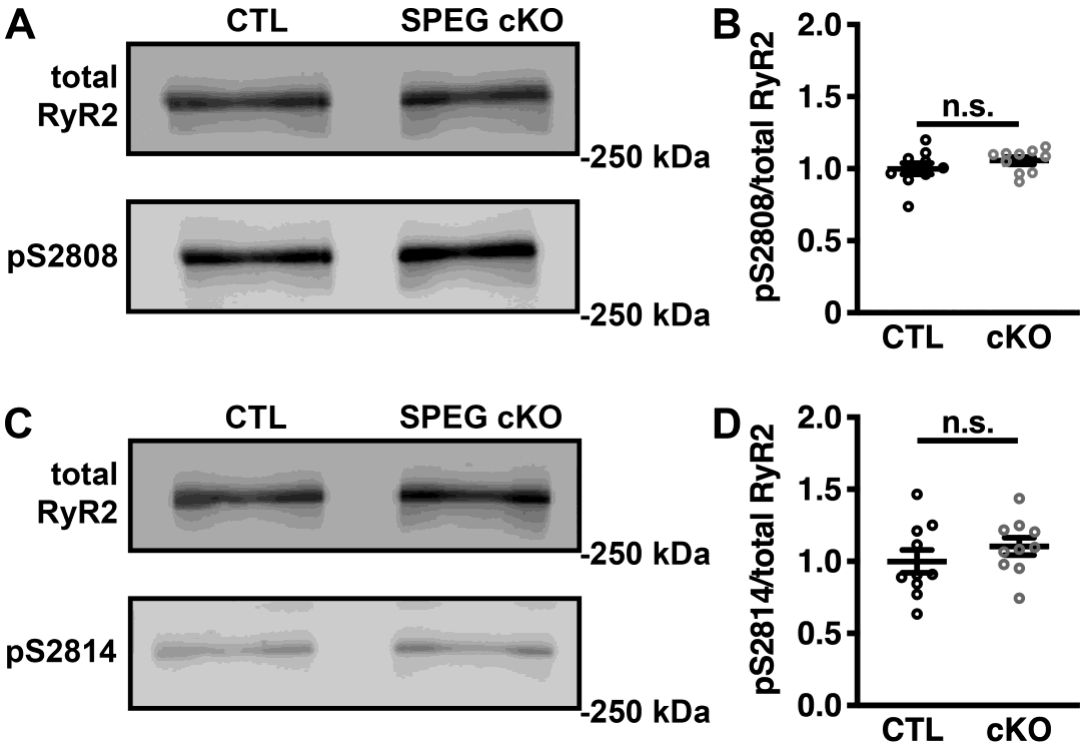

Figure VII. RyR2-S2808 and RyR2-S2814 phosphorylation are unchanged in SPEG cKO mice. (A) Representative western blot of RyR2-pS2808 and total RyR2 in SPEG cKO and CTL hearts. **(B)** Bar graph quantifying pS2808 relative to total RyR2 in SPEG cKO vs CTL hearts. (**C)** Representative western blot of RyR2-pS2814 and total RyR2 in SPEG cKO and CTL hearts. **(D)** Bar graph quantifying pS2814 relative to total RyR2 in SPEG cKO vs CTL hearts. Statistical analyses performed using the Student's t-test. n.s.= no significance.

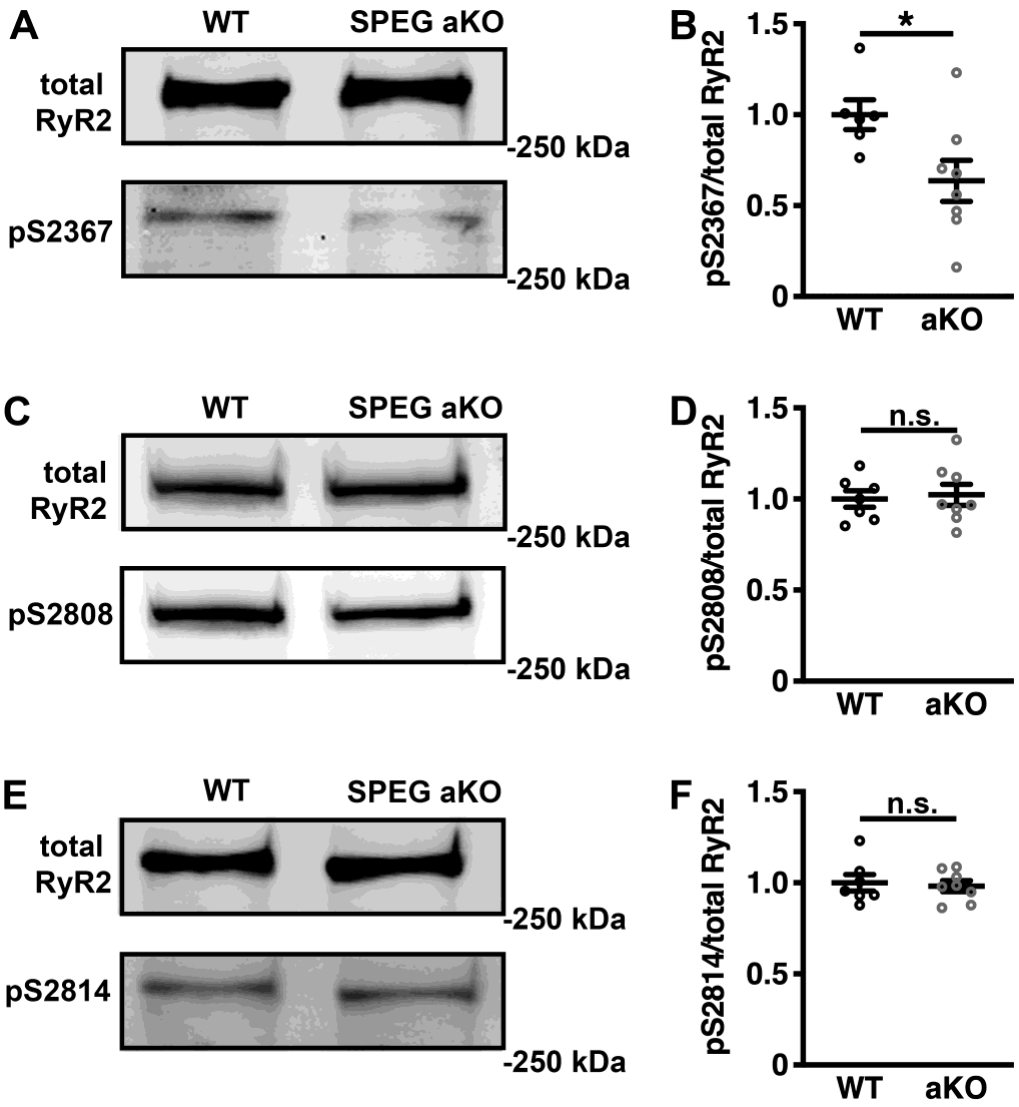

Figure VIII. RyR2-S2367 phosphorylation is decreased in SPEG atrial KO (aKO) mice. (A) Representative western blot image showing pS2367 and total RyR2 levels in SPEG aKO and WT atria. **(B)** Bar graph showing decreased pS2367 relative to total RyR2 in SPEG aKO vs WT atria. **(C)** Representative western blot image showing pS2367 and total RyR2 levels in SPEG aKO and WT atria. **(D)** Bar graph showing no change in pS2808 relative to total RyR2 levels in SPEG aKO atria. **(E)** Representative western blot image showing pS2814 and total RyR2 levels in SPEG aKO and WT atria. **(F)** Bar graph showing no change in pS2814 relative to total RyR2 levels in SPEG aKO atria. Statistical analyses performed with Mann-Whitney U test. *P<0.05.

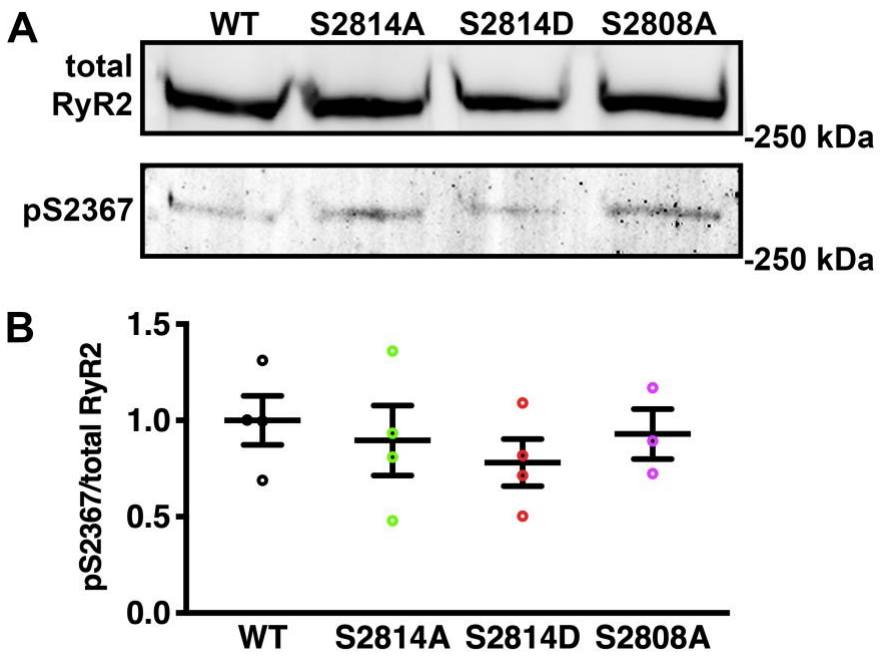

Figure IX. RyR2-S2367 phosphorylation is unaffected by RyR2-S2808 or RyR2-S2814 phosphorylation. (A) Representative western blot image showing pS2367 and total RyR2 in WT, RyR2-S2814A, RyR2-S2814D, and RyR2-S2808A atria **(B)** Bar graph showing no change in pS2367 relative to total RyR2 between WT, RyR2-S2814A, RyR2-S2814D, and RyR2-S2808A atria. Statistical analyses performed with Kruskall-Wallis test.

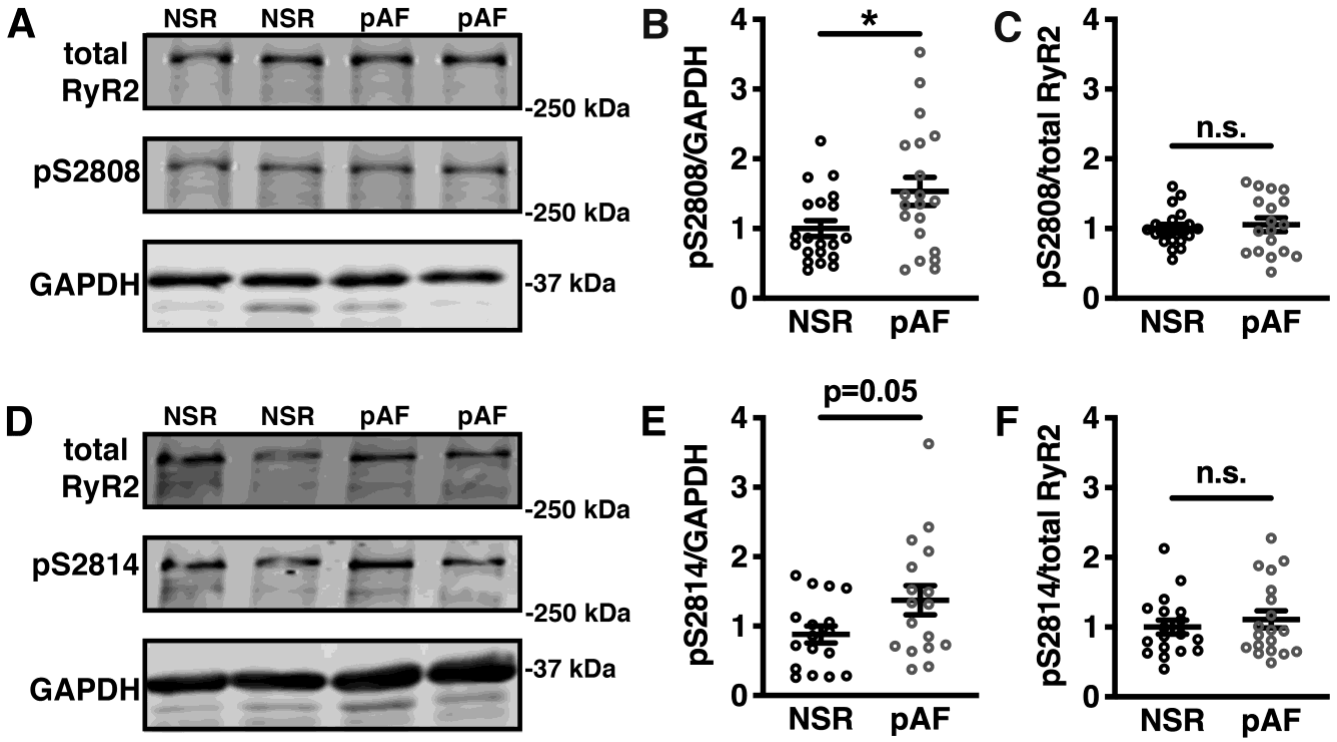

Figure X. RyR2-S2808 and RyR2-S2814 phosphorylation in pAF patients. (A) Representative Western blot image of total RyR2, pS2808 and GAPDH (loading control) in right atrial appendage samples from patients in normal sinus rhythm (NSR) and paroxysmal AF (pAF). (**B**) Bar graph showing increased RyR2-pS2808 levels relative to GAPDH in pAF vs NSR samples. (**C**) Bar graph showing no change in RyR2-pS2808 relative to total RyR2 in pAF vs NSR samples. (**D**) Representative Western blot image of total RyR2, pS2814 and GAPDH in NSR and pAF samples. (**E**) Bar graph showing increased RyR2-pS2814 relative to GAPDH in pAF vs NSR samples. (**F**) Bar graph showing no change in RyR2-pS2814 relative to total RyR2 in pAF vs NSR samples. Statistical analyses performed with the Student's t-test. *P<0.05.

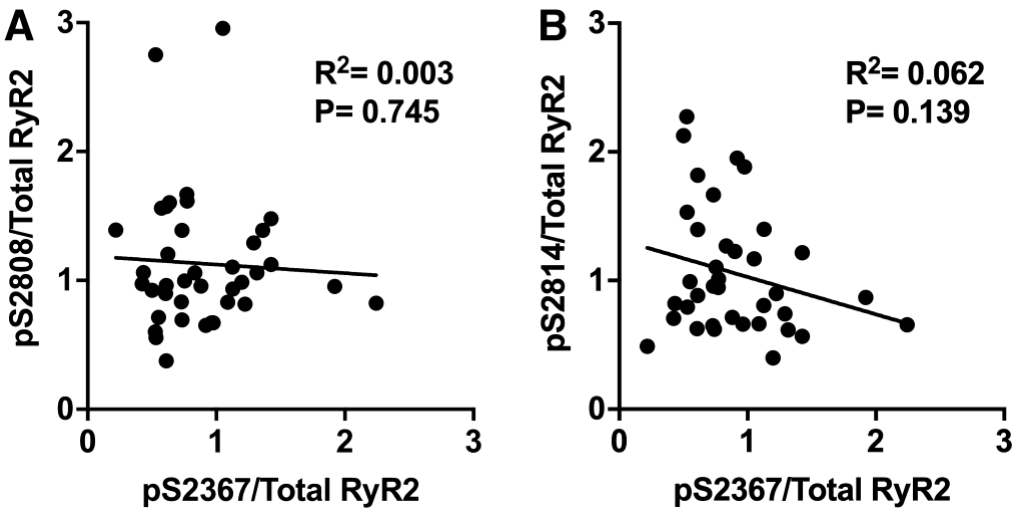

Figure XI. Lack of correlation of S2367 phosphorylation with S2808 and S2814 phosphorylation in human atrial samples. Scatter plots showing lack of correlation between S2367 phosphorylation on RyR2 and S2808 (**A**) or S2814 (**B**) phosphorylation levels normalized to total RyR2 in human atrial biopsies from patients undergoing cardiac surgery. Statistical analysis performed using Pearson correlation.

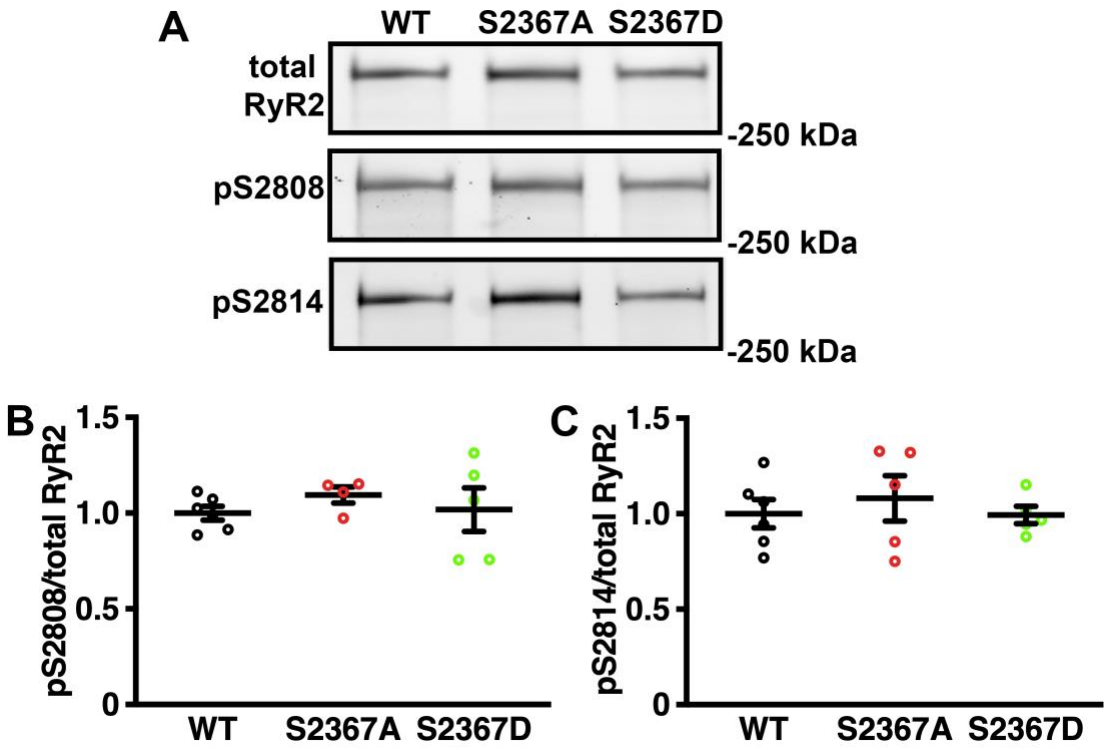

Figure XII. RyR2-S2808 and RyR2-S2814 phosphorylation are unchanged in atria from RyR2-S2367A and RyR2-S2367D mice. (A) Representative western blot image showing pS2814, pS2808 and total RyR2 in WT, S2367A, and S2367D atria. **(B)** Bar graph showing no change in pS2808 relative to total RyR2 between WT, S2367A, and S2367D atria. **(C)** Bar graph showing no change in pS2814 relative to total RyR2 between WT, S2367A, and S2367D atria. Statistical analyses performed with Kruskall-Wallis test.

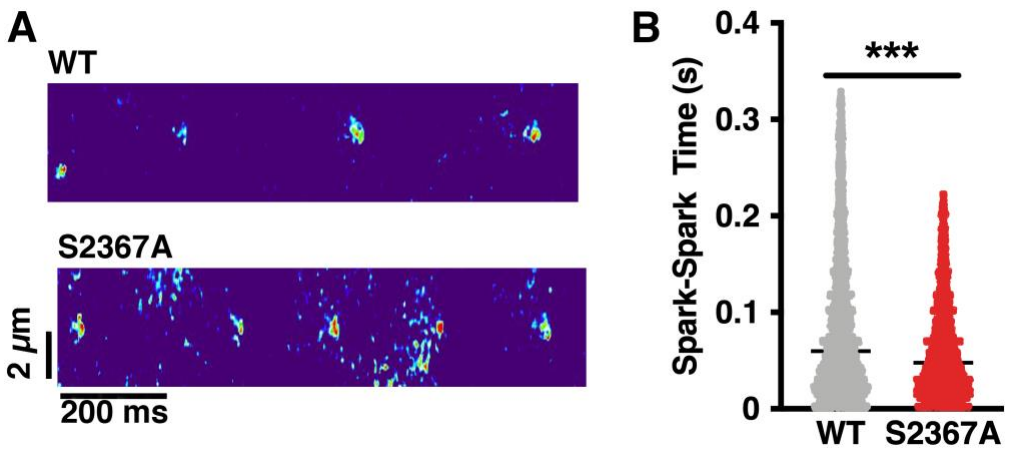

Figure XIII. Mouse RyR2-S2367A channel have decreased spark latency time. (A) Representative confocal images showing repeated sparks from individual RyR2 cluster after treatment with ryanodine (50 nM). **(B)** Median and scatter of spark-spark delays in WT (n=3 mice, 6372 spark pairs) and S2367A (n=3 mice, 6913 spark pairs) atrial myocytes. Data analyzed statistically with Kolmogorov-Smirnov test. ***P<0.0001.